Supporting Information

Anthraquinone-based covalent organic framework for highly reversible aqueous zinc-ion batteries cathode

Lihua Li*†[a], Haohao Yang†[a], Xin Wang[a], Yinghu Ma[a], Weizhi Ou[a], Hui Peng*[a], Guofu Ma*[a]

[a] Key Laboratory of Eco-functional Polymer Materials of the Ministry of Education, Key Laboratory of Polymer Materials Ministry of Gansu Province, College of Chemistry and Chemical Engineering, Northwest Normal University, Lanzhou 730070, China.

* E-mail: lilh2019@nwnu.edu.cn; penghui@nwnu.edu.cn; magf@nwnu.edu.cn

† The authors contributed equally to this work.

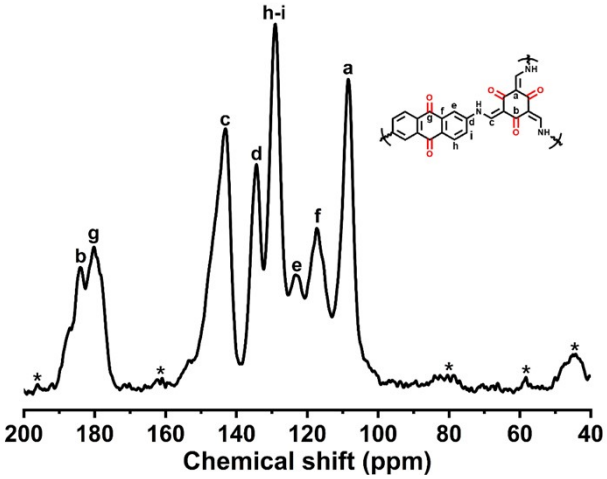

Figure S1. Solid-state ^{13}C CP/MAS NMR of TfDa-COF.

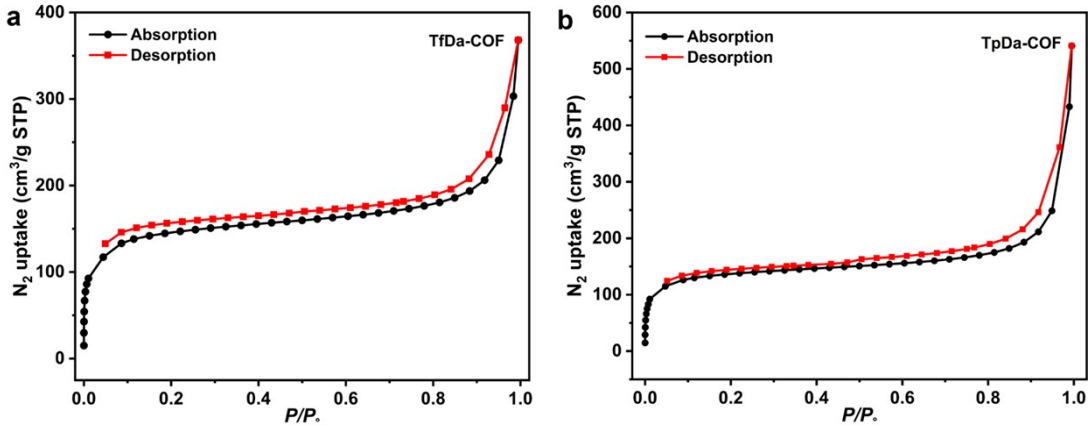

Figure S2. (a, b) N_2 adsorption and desorption isotherms of TfDa-COF and TpDa-COF.

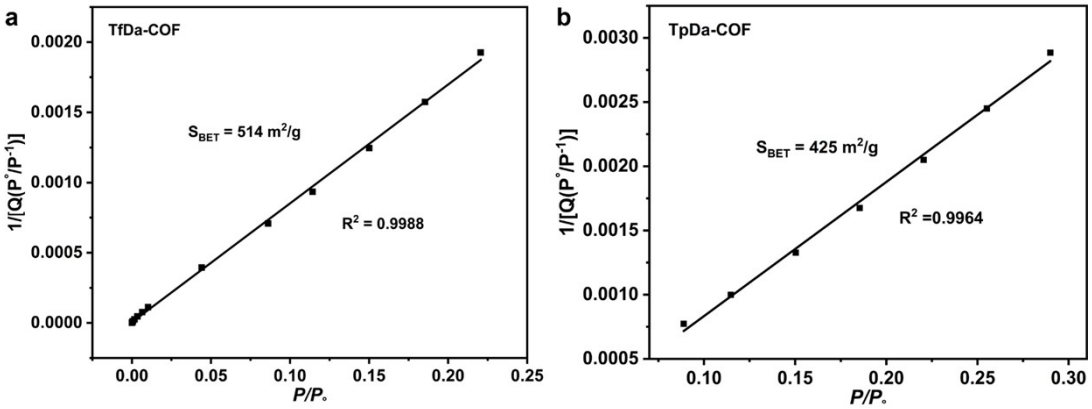

Figure S3. (a, b) Specific surface area of TfDa-COF and TpDa-COF.

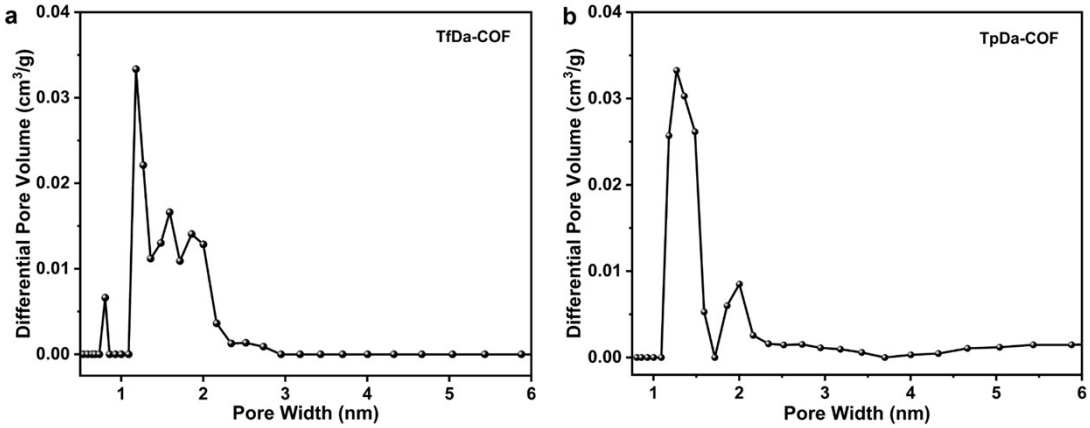

Figure S4. (a, b) Pore size distribution of TfDa-COF and TpDa-COF.

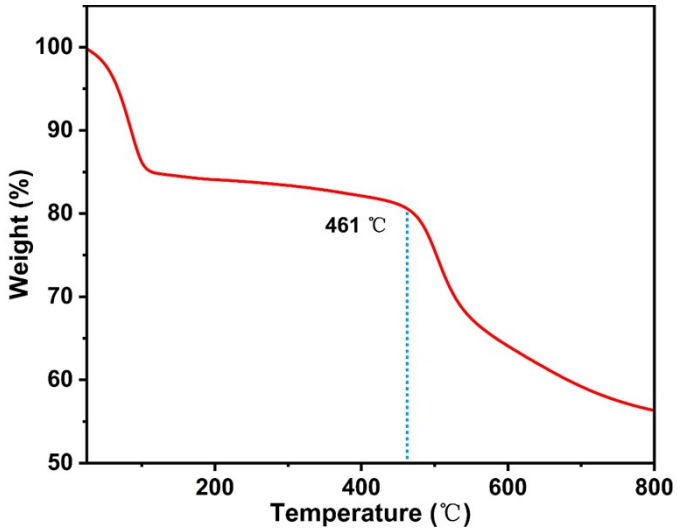

Figure S5. TGA curve of TfDa-COF.

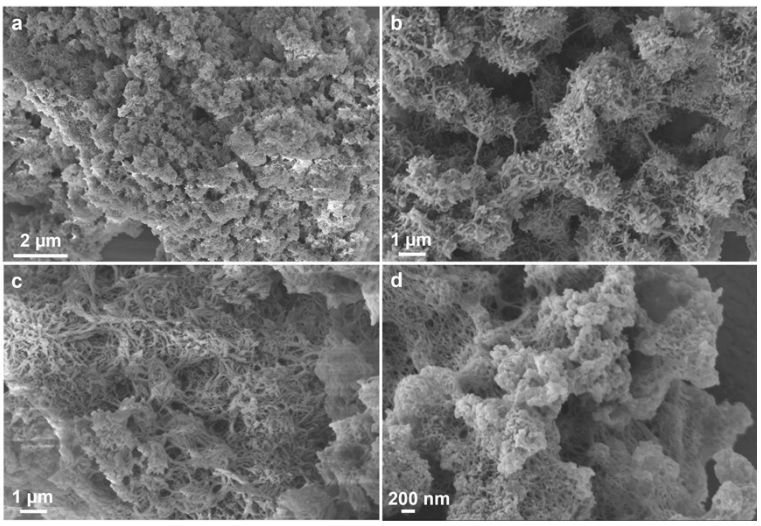

Figure S6. (a-d) SEM images of TfDa-COF at different magnifications.

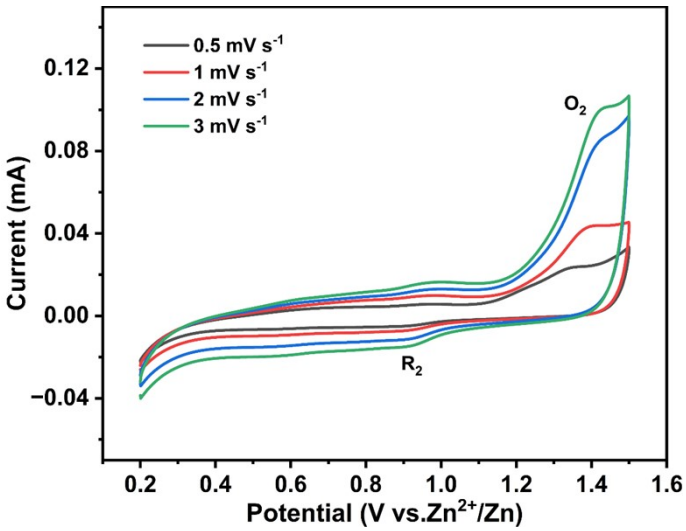

Figure S7. CV curves of Zn//TpDa-COF battery at different scan rates.

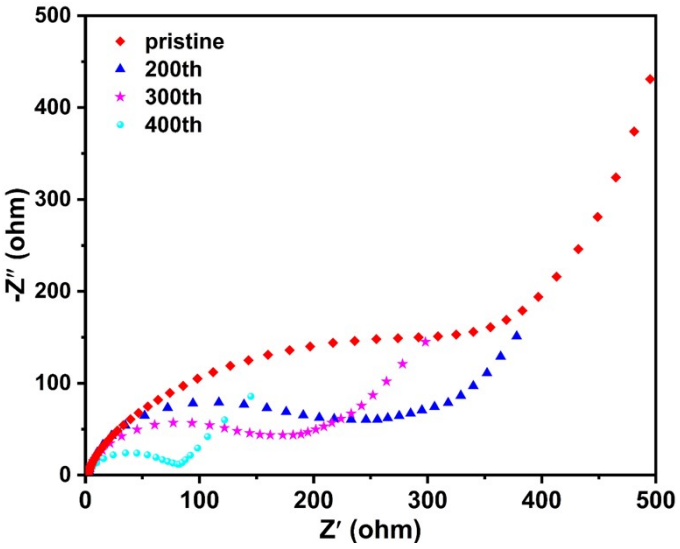

Figure S8. The EIS of TfDa-COF.

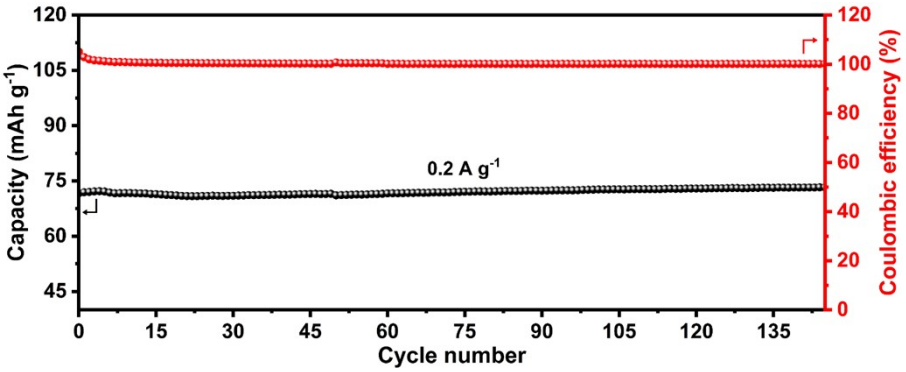

Figure S9. The short-cycle stability performance of the TfDa-COF tested at 0.2 A g^{-1}.

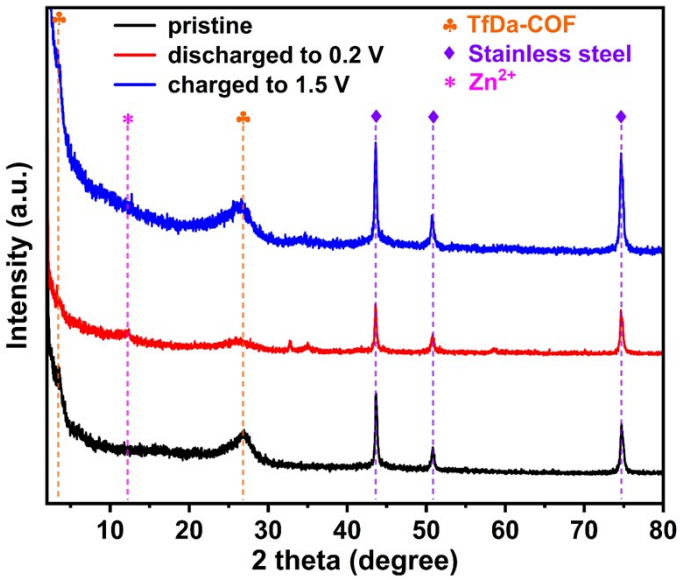

Figure S10. PXRD test of TfDa-COF cathode in pristine, fully discharged and fully charged states.

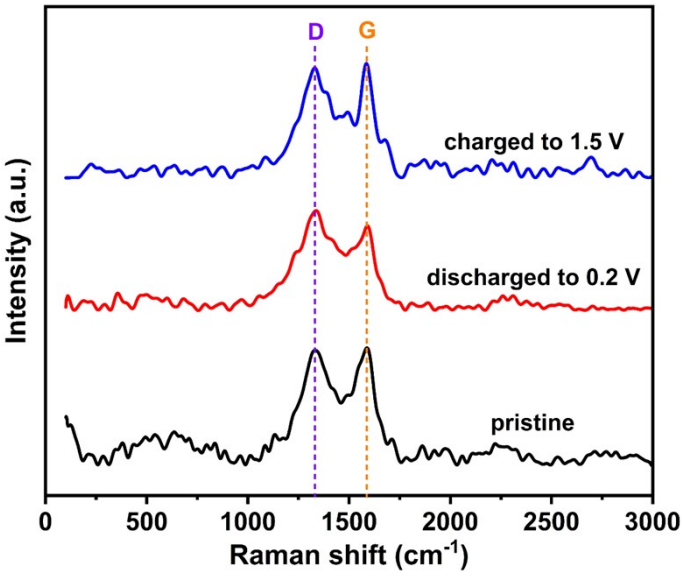

Figure S11. Raman test of TfDa-COF cathode in pristine, fully discharged and fully charged states.

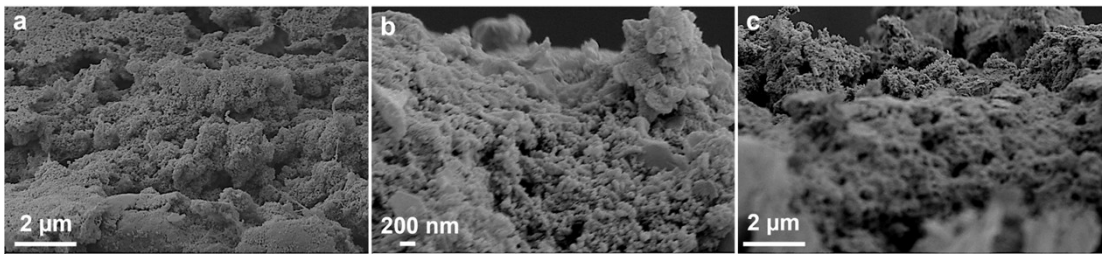

Figure S12. SEM images of TfDa-COF cathode cross-sections during the charge discharge process. (a) pristine, (b) fully discharged, and (c) fully recharged states after 100 cycles.

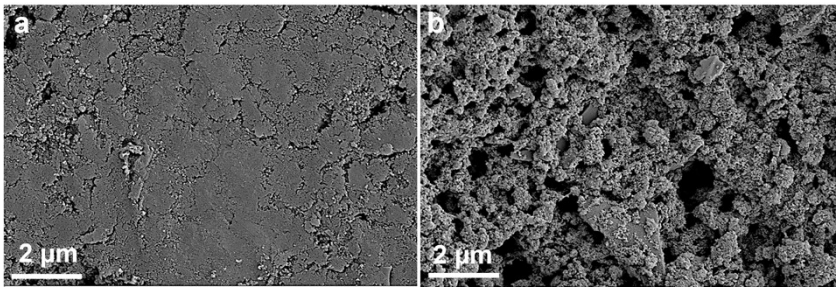

Figure S13. The surface morphology of TfDa-COF cathode at pristine state.

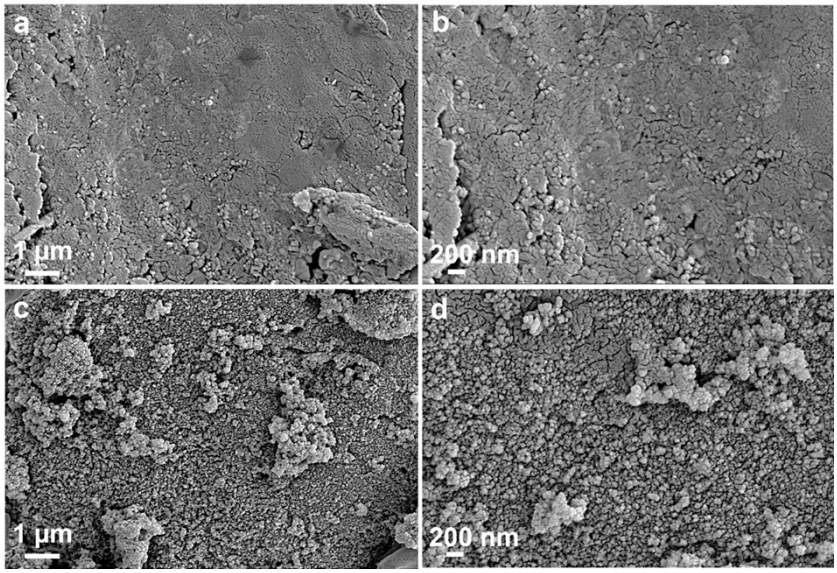

Figure S14. SEM images of TfDa-COF cathode surface after 100 cycles. (a, b) fully discharged state, (c, d) fully recharged state.

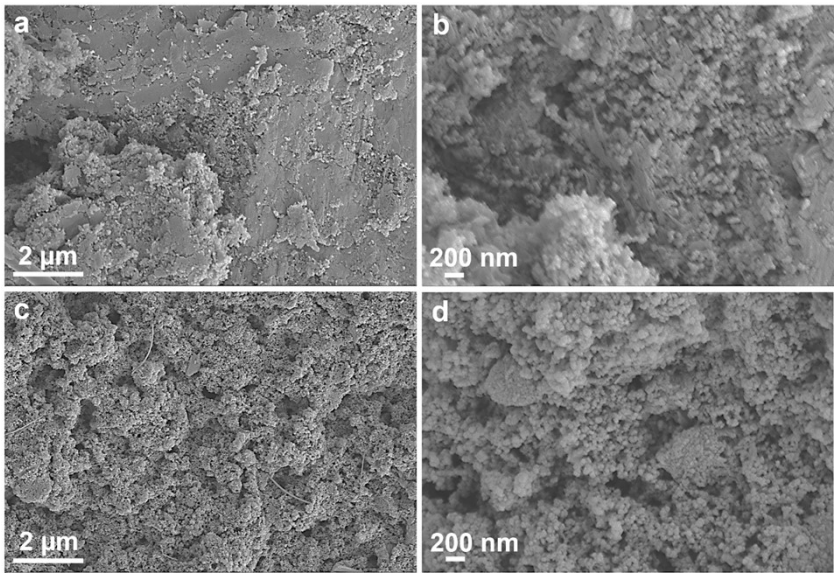

Figure S15. SEM images of TfDa-COF cathode surface after 1000 cycles. (a, b) fully discharged state, (c, d) fully recharged state.

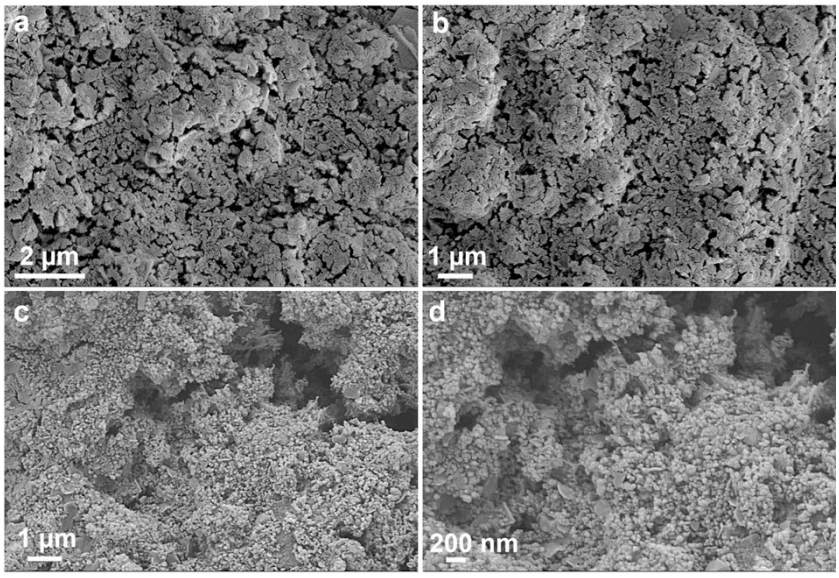

Figure S16. SEM images of TfDa-COF cathode surface after 10000 cycles. (a, b) fully discharged state, (c, d) fully recharged state.

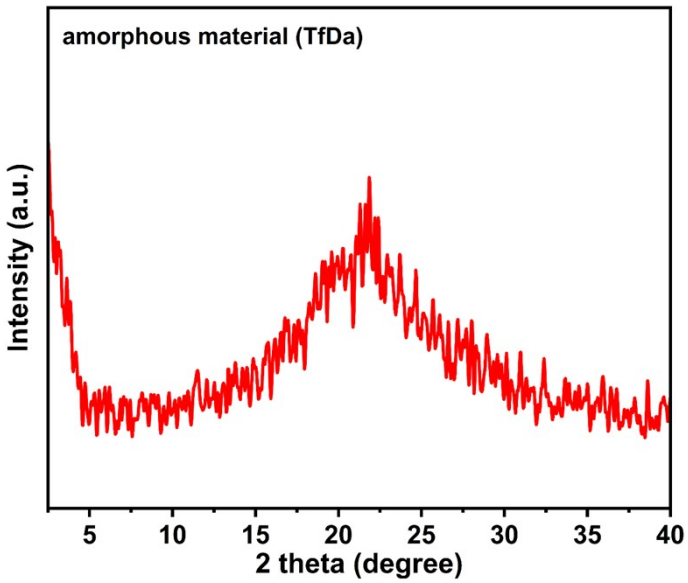

Figure S17. PXRD patterns of amorphous material TfDa.

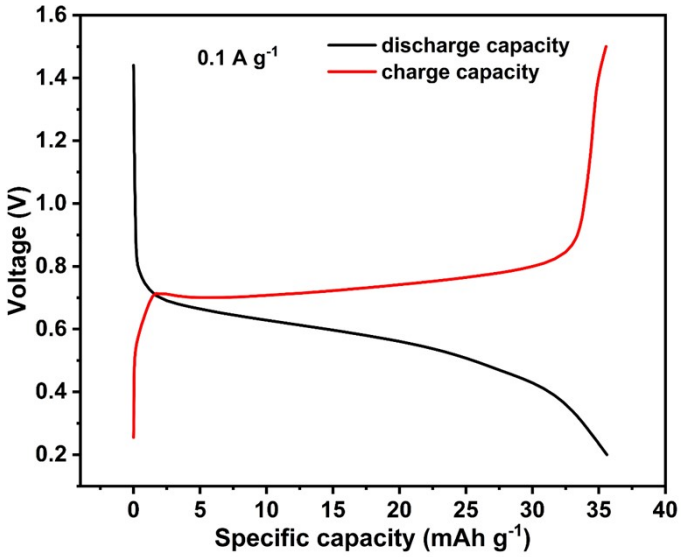

Figure S18. The GCD curves of TfDa under 0.1 A g^{-1}.

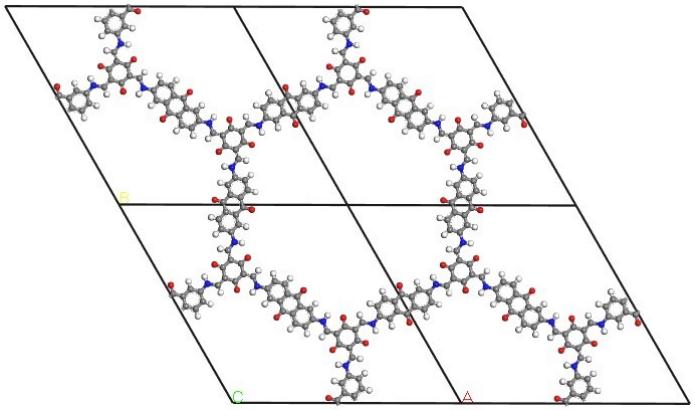

Figure S19. Simulated crystalline structure of TfDa-COF.

The structure of TfDa-COF was obtained by Materials Studio 8.0 simulation, and the cell volume of TfDa-COF was obtained as 2.79×10^{-27} m^3 through the simulation of the structure, so that we obtained V_M (1.68×10^{-3} m^3 mol^{-1}) = cell volume (2.79×10^{-27} m^3) × N_A.

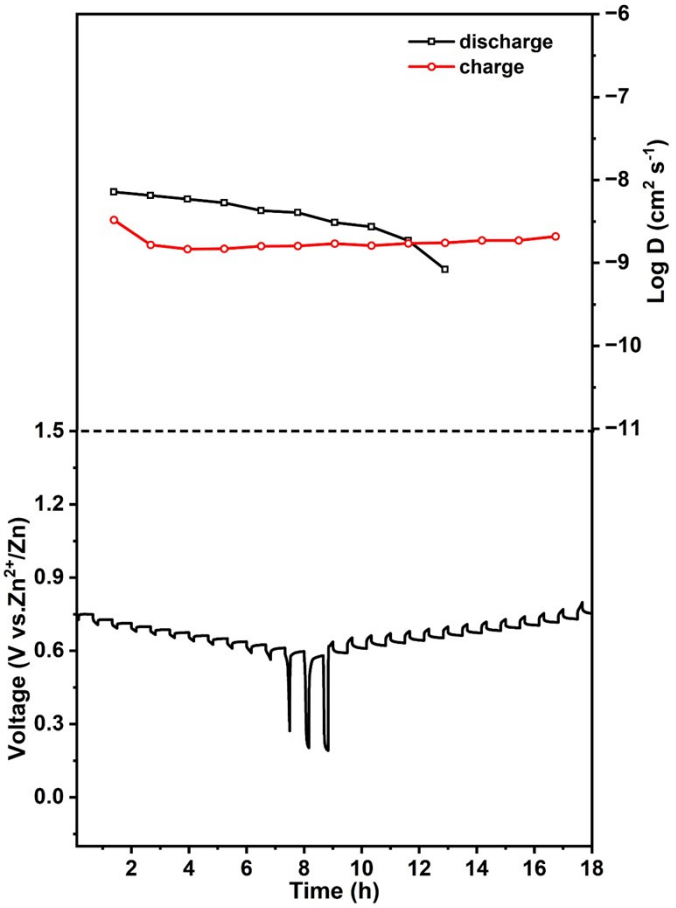

Figure S20. The GITT curves and calculated diffusion coefficients of TfDa-COF during cycling under 0.03 A g^{-1}.

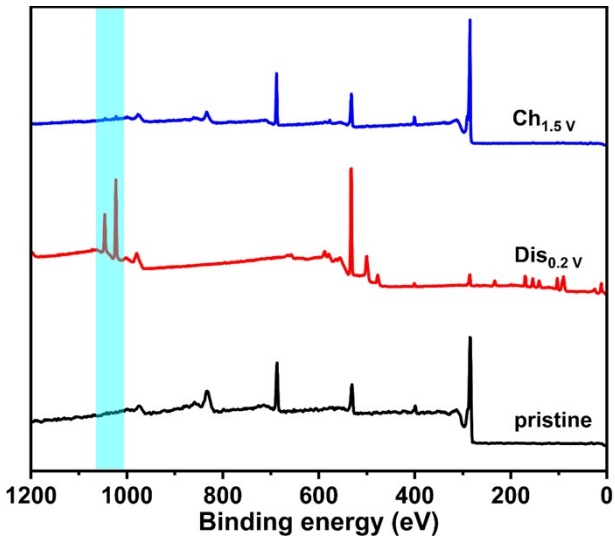

Figure S21. XPS spectra of TfDa-COF electrode at pristine, fully discharged (0.2 V), and fully charged (1.5 V) states.

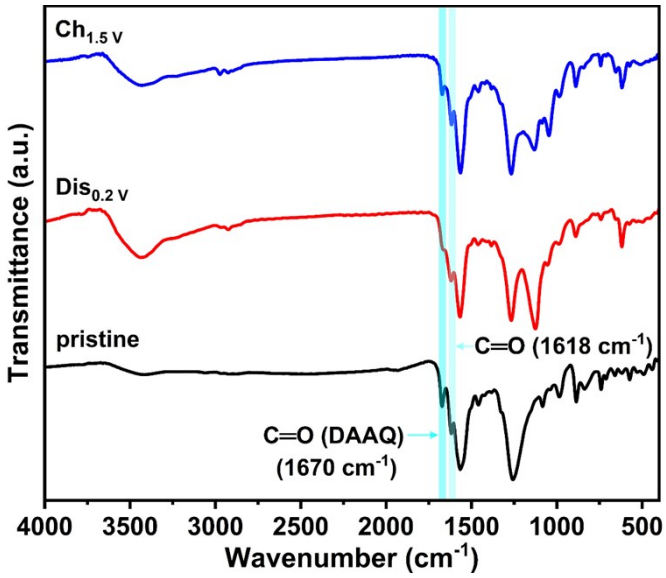

Figure S22. FT-IR spectra of TfDa-COF electrode at pristine, fully discharged (0.2 V), and fully charged (1.5 V) states.

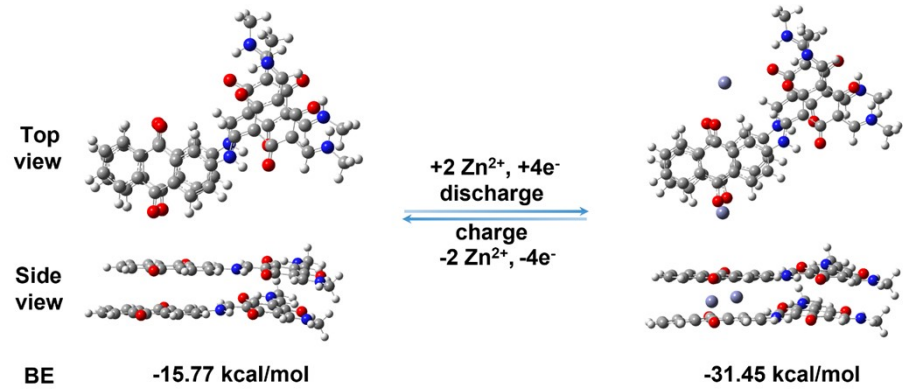

Figure S23. The DFT models of Zn_2@TfDa-COF.

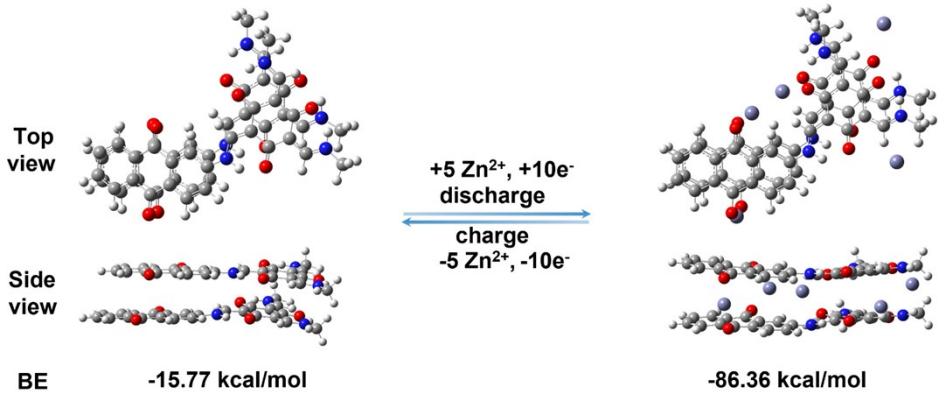

Figure S24. The DFT models of Zn_5@TfDa-COF.

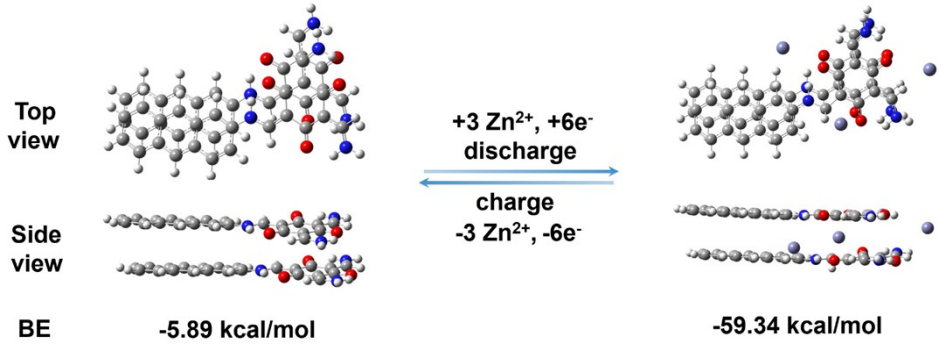

Figure S25. The DFT models of Zn_3@TpDa-COF.

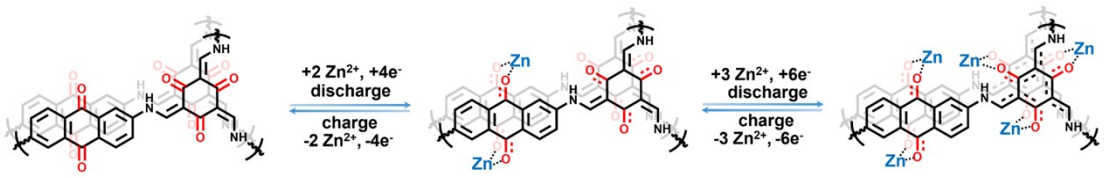

Figure S26. The possible mechanism of the interaction of Tp-PTO-COF with Zn^{2+} ions during the charge-discharge process.

Table S1. Comparative electrochemical performance of TfDa-COF and other reported cathode materials for aqueous ZIBs.

Material type	Cathode material	Electrolyte	Voltage (V)	Retention (%/no. of cycle)	Reference
Inorganic compounds	δ-MnO_2	0.5 M $ANZn(TFSI)_2$	0.05-1.9	60/100 (0.04 C)	1
	CuHCF	1 M $ZnSO_4$	0.8-1.9	77/20 (20 mA g^{-1})	2
	Todorokite[3×3]	1 M $ZnSO_4$	0.7-2.0	95/50 (0.2 C)	3
	$V_{0.91}Al_{0.05}O_{1.52}(OH)_{0.77}$	1 M $ZnSO_4$	0.2-1.13	67/50 (15 mA g^{-1})	4
	Mo_6S_8	1 M $ZnSO_4$	0.25-1.0	95/150 (180 mA g^{-1})	5
	VS_2	1 M $ZnSO_4$	0.4-1.0	98/200 (0.5 A g^{-1})	6
	Ni-PTA-Mn	3 M $ZnSO_4$ 0.2 M $MnSO_4$	0.8-1.8	93/100 (1 A g^{-1})	7
Organic compounds	IDAQ/rGO	3 M Zn $(CF_3SO_3)_2$	0.2-1.8	33/5000 (2 A g^{-1})	8
	Ni-Ndi-trz	2 M $ZnSO_4$	0.3-1.6	80/500 (3 A g^{-1})	9
	TCNAQ	2 M $ZnSO_4$	0.6-1.8	81/1000 (0.5 A g^{-1})	10
	PDA	3.3 M $ZnSO_4$	0.3-1.4	96/500 (200 mA g^{-1})	11
	π-PMC	2 M $ZnCl_2$	0.05-1.0	68.2/1000 (8 A g^{-1})	12
	PDpBQ	2 M $ZnSO_4$	0.9-1.6	78/500 (2 A g^{-1})	13
COFs	HqTp-COF	3 M $ZnSO_4$	0.2-1.8	95/1000 (3.75 A g^{-1})	14
	PA-COF	1 M $ZnSO_4$	0.2-1.6	62/10000 (10 A g^{-1})	15
	HA-COF	2 M $ZnSO_4$	0.2-1.6	75/10000 (5 A g^{-1})	16
	HAQ-COF	2 M $ZnSO_4$	0.2-1.6	88/10000 (5 A g^{-1})	16
	TP-PTO-COF	2 M $ZnSO_4$	0.4-1.5	95/1000 (2 A g^{-1})	17
	TfDa-COF	2 M $ZnSO_4$	0.2-1.5	98/10000 (2.5 A g^{-1})	This work

Table S2. Comparison of diffusion coefficients of TfDa-COF with reported cathode materials for aqueous ZIBs.

Materials	Diffusion coefficient (D_{Zn}^{2+}) ($cm^2\ s^{-1}$)	Reference
MnO_2	10^{-10}-10^{-13}	18
V_4O_9	4×10^{-11}-2.4×10^{-10}	19
CLPy	9.3×10^{-12}-1.3×10^{-9}	20
PDBS	10^{-11}-10^{-10}	21
DQDPD	10^{-10}-10^{-9}	22
PA-COF	10^{-11}-10^{-8}	15
TfDa-COF	10^{-9}-10^{-8}	This work

Theoretical capacity

The theoretical specific capacity = $\frac{No.of\ electrons\ \times 96485}{3600\ \times Molecular\ weight}$ [14, 17]

There are 24 carbonyl groups as active sites in the unit cell, based on bilayer model fragment compound, each Zn^{2+} coordinates with two oxygen atoms between the layers to form an O···Zn···O bond during the discharge process. Therefore, maximum number of Zn^{2+} ions interacted in the unit cell of TfDa-COF = 12.

Number of electrons from one Zn^{2+} ion = 2

Total number of electrons = 24

Molecular weight of the monolayer TfDa-COF = 1020 g mol^{-1}

Therefore, the theoretical specific capacity = $\frac{24\ \times\ 96485}{3600\ \times\ 1020\ \times\ 2}$ = 0.315 Ah g^{-1} = 315 mAh g^{-1}.

References

1 S.-D. Han, S. Kim, D. Li, V. Petkov, H. D. Yoo, P. J. Phillips, H. Wang, J. J. Kim, K. L. More, B. Key, R. F. Klie, J. Cabana, V. R. Stamenkovic, T. T. Fister, N. M. Markovic, A. K. Burrell, S. Tepavcevic and J. T. Vaughey, *Chem. Mater.*, 2017, **29**, 4874-4884.

2 Z. Jia, B. Wang and Y. Wang, *Mater. Chem. Phys.*, 2015, **149-150**, 601-606.

3 J. Lee, J. B. Ju, W. I. Cho, B. W. Cho and S. H. Oh, *Electrochim. Acta*, 2013, **112**, 138-143.

4 J. H. Jo, Y.-K. Sun and S.-T. Myung, *J. Mater. Chem. A*, 2017, **5**, 8367-8375.

5 Y. Cheng, L. Luo, L. Zhong, J. Chen, B. Li, W. Wang, S. X. Mao, C. Wang, V. L. Sprenkle, G. Li and J. Liu, *ACS Appl. Mater. Interfaces*, 2016, **8**, 13673-13677.

6 P. He, M. Yan, G. Zhang, R. Sun, L. Chen, Q. An and L. Mai, *Adv. Energy Mater.*, 2017, **7**, 1601920.

7 C. Li, C. Zheng, H. Jiang, S. Bai and J. Jia, *J. Alloys Compd.*, 2021, **882**, 160587.

8 X. Geng, Y. Jiang, H. Ma, H. Zhang, J. Liu, Z. Zhang, C. Peng, J. Zhang, Q. Zhao and N. Zhu, *ACS Appl. Mater. Interfaces*, 2022, **14**, 49746-49754.

9 Y. Liu, Z. Li, Y. Han, Z. Ji, H. Li, Y. Liu, Y. Wei, C. Chen, X. He and M. Wu, *ChemSusChem*, 2023, **16**, e202202305.

10 Q. Wang, X. Xu, G. Yang, Y. Liu and X. Yao, *Chem. Comm.*, 2020, **56**, 11859-11862.

11 X. Yue, H. Liu and P. Liu, *Chem. Comm.*, 2019, **55**, 1647-1650.

12 H. Zhang, Y. Fang, F. Yang, X. Liu and X. Lu, *Energy Environ. Sci.*, 2020, **13**, 2515-2523.

13 X. Wang, J. Xiao and W. Tang, *Adv. Funct. Mater.*, 2021, **32**, 2108225.

14 M. A. Khayum, M. Ghosh, V. Vijayakumar, A. Halder, M. Nurhuda, S. Kumar, M. Addicoat, S. Kurungot and R. Banerjee, *Chem. Sci.*, 2019, **10**, 8889-8894.

15 W. Wang, V. S. Kale, Z. Cao, S. Kandambeth, W. Zhang, J. Ming, P. T. Parvatkar, E. Abou-Hamad, O. Shekhah, L. Cavallo, M. Eddaoudi and H. N. Alshareef, *ACS Energy Lett.*, 2020, **5**, 2256-2264.

16 W. Wang, V. S. Kale, Z. Cao, Y. Lei, S. Kandambeth, G. Zou, Y. Zhu, E. Abouhamad, O. Shekhah, L. Cavallo, M. Eddaoudi and H. N. Alshareef, *Adv. Mater.*, 2021, **33**, e2103617.

17 D. Ma, H. Zhao, F. Cao, H. Zhao, J. Li, L. Wang and K. Liu, *Chem. Sci.*, 2022, **13**, 2385-2390.

18 Y. Zhao, P. Zhang, J. Liang, X. Xia, L. Ren, L. Song, W. Liu and X. Sun, *Energy Stor. Mater.*, 2022, **47**, 424-433.

19 Q. Wang, T. Sun, S. Zheng, L. Li, T. Ma and J. Liang, *Inorg. Chem. Front.*, 2021, **8**, 4497-4506.

20 C. Zhang, W. Ma, C. Han, L.-W. Luo, A. Daniyar, S. Xiang, X. Wu, X. Ji and J.-X. Jiang, *Energy Environ. Sci.*, 2021, **14**, 462-472.

21 T. Sun, Z. J. Li, Y. F. Zhi, Y. J. Huang, H. J. Fan and Q. Zhang, *Adv. Funct. Mater.*, 2021, **31**, 2010049.

22 H. Peng, J. Xiao, Z. Wu, L. Zhang, Y. Geng, W. Xin, J. Li, Z. Yan, K. Zhang and Z. Zhu, *CCS Chemistry*, 2022, **5**, 1789-1801.